JOURNAL OF MATERIALS SCIENCE 18 (1983) 2905–2914

Microstructural characterization of doped dicalcium silicate polymorphs

A. GHOSE, S. CHOPRA*, J. F. YOUNG
Departments of Civil Engineering and Ceramic Engineering, University of Illinois, Urbana, Illinois 61801, USA

This study has shown that both β- and α'-C_2S can be readily stabilized by suitable doping with BaO, B_2O_3, and P_2O_5, using a single firing at 1450° C. The β-C_2S samples all have similar lamellar structures, irrespective of the dopant present, which show (100) twinning. Grain boundary phases are present in all β-C_2S preparations. The α'-C_2S crystals usually contain precipitates and associated strain fields and dislocations, but a grain boundary phase was only observed in α'-C_2S stabilized by BaO. Some correlation between reactivity and presence of dislocations and strain fields has been suggested for the α'-C_2S phase.

1. Introduction

Dicalcium silicate (C_2S) is an important compound in several fields of silicate science; e.g. cements, refractories and slags. It exhibits polymorphism and at least five well-documented forms have been reported [1, 2]. The exact scheme of transformation is not yet fully agreed on in the literature [1, 2], however the latest contribution [3] simplified the scheme somewhat:

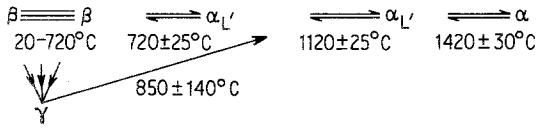

The $\beta \rightleftharpoons \alpha'_L$ and $\alpha'_L \rightleftharpoons \alpha'_H$ transformations are both displacive and the transformation enthalpies are smaller (1423 to 2720 and 720 J mol^{-1} respectively) [2] than that for the $\alpha'_H \rightleftharpoons \alpha$ transformation (13.5 to 14.2 kJ mol^{-1}), which is semi-reconstructive. Except for the γ-form, which is stable at room temperature, the other polymorphs are stable in their pure state only at elevated temperatures, although these may be stabilized at ambient temperature by the incorporation of suitable dopants into their crystal lattices. It is the β-form that is commonly found in commercial Portland cement. The polymorphs exhibit differing hydraulic activity towards water, with the γ-form being the least hydraulic. Attempts to produce more "reactive" forms of C_2S (or belite) involve the use of various thermal treatments [4–6] and different stabilizers [7–10]. In a collaborative study [8–10], it has been observed that the hydraulic activity and strength development of BaO- and P_2O_5- and α'-doped β-belites increase in the order of α'-C_2S(BaO) > β-C_2S(BaO) > α'-C_2S(P_2O_5) > β-C_2S(P_2O_5). Microstructural characterization of similar P_2O_5-, BaO-, and B_2O_3-doped belites using electron-optical methods were undertaken to gain insight into the probable causes of such differences and the results are discussed in this paper.

2. Experimental details

The belites under study were prepared [11] from reagent grade chemicals, varying the dopant concentration to stabilize the α' or the β polymorph. In either case, the compositions were based on a CaO/SiO_2 ratio of 2.0 after accounting for the dopant substitutions. The starting compositions which are given in Table I, were selected on the basis of previous studies [8, 12, 13]. The charges were wet ground and homogenized in a ball mill, followed by dry milling and calcining at 1000° C for 90 min. They were further dry milled, compacted into pellets at 2.8×10^8 Pa, and fired twice

*Present address: Advanced Micro Devices, Sunnyvale, Ca 94086, USA.

0022–2461/83 $03.00 + .12

TABLE I Compositional analyses of the polymorphs as calculated, as chemically analysed (atomic absorption) and as analysed by the EDS analyses

Polymorph		CaO	SiO_2	BaO	P_2O_5	B_2O_3	SO_3	Al_2O_3	Fe_2O_3	K_2O	MgO	Total	C/S
BaO β	Initial	63.30	34.51	2.19	–	–	–	–	–	–	–	100.00	1.99
	Final	60.87	33.89	2.55	–	–	–	0.32	0.01	–	0.04	97.65	1.95
	Probe	62.59	33.94	2.21	0.08	–	0.07	0.10	0.02	0.04	0.01	99.09	2.02
BaO α'	Initial	56.32	32.47	11.21	–	–	–	–	–	–	–	100.00	1.99
	Final	54.30	30.98	8.12	–	–	–	0.71	0.07	–	–	94.18	1.98
	Probe	57.23	32.80	9.87	0.08	–	0.08	0.09	–	0.07	0.04	100.27	1.99
B_2O_3 β	Initial	65.50	33.50	–	–	1.00	–	–	–	–	–	100.00	1.99
	Final	63.48	33.20	–	–	0.13	–	0.16	0.04	–	–	97.01	2.03
	Probe	63.93	33.10	0.02	0.07	–	0.06	0.05	0.04	0.08	0.04	(97.39)	–
B_2O_3 α'	Initial	66.46	30.54	–	–	3.00	–	–	–	–	–	100.00	1.99
	Final	63.03	29.44	–	–	0.65	–	0.13	0.04	–	–	93.29	2.20
	Probe	64.34	31.78	0.04	0.06	–	0.06	0.03	0.02	0.09	0.05	(96.47)	–
P_2O_5 β	Initial	64.60	31.36	–	4.04	–	–	–	–	–	–	100.00	1.99
	Final	61.57	30.72	–	1.20	–	–	0.14	0.04	–	–	93.67	2.08
	Probe	64.54	34.05	0.04	0.54	–	0.06	0.06	0.03	0.07	0.05	99.44	2.02
P_2O_5 α	Initial	62.50	32.00	–	5.50	–	–	–	–	–	–	100.00	1.99
	Final	62.97	29.27	–	4.90	–	–	0.23	0.01	–	–	97.38	2.02
	Probe	63.28	31.61	0.04	3.06	–	0.08	0.06	0.01	0.02	0.02	98.51	1.99

at 1450° C for 90 min, with intermediate grinding and repelletizing.

X-ray powder patterns of the sintered material after each firing (using a Phillips Norelco diffractometer) indicated satisfactory phase purity in that, in all cases, the desired polymorph was found to have been stabilized. It was determined that the second firing was not really necessary. For the α'-C_2S preparations, however, a small amount of β-C_2S was also found (< 5%), which persisted after the second firing. The α'-C_2S patterns agree well with published data [2]; splitting of the 0.274 nm peak when B_2O_3 is present as reported by Suzuki and Yamaguchi [12], was confirmed. The P_2O_5-doped α'-C_2S showed much broader diffraction peaks than did the other samples. All doped β-C_2S samples gave patterns which were similar to that reported for pure β-C_2S.

The stabilized belites were examined using a number of methods. X-ray powder photography was undertaken to find the lattice parameters of the various preparations. These results will be reported separately. A Dupont differential thermal analyser (Model 1090) was used to find out any changes in the transformation temperatures of the polymorphs consequent on varying levels of different dopants. Electron microprobe analysis (EMPA) [JEOL 50X equipped with an energy dispersive spectrometer (EDS)], was employed to estimate the extent of actual dopant uptake in the belite grains, and also to analyse any second phases present. Scanning electron microscopy (SEM) was used (JEOL JSM-U3) in conjunction with progressive etching of cut and polished specimens with 0.5% nital to qualitatively evaluate the degree of reactivity of the different belites. These etching studies have been reported elsewhere [14]. Transmission electron microscopy (TEM) was undertaken to study the microstructure at a finer level than is possible with SEM. Specimens for TEM were prepared by ion-milling mechanically-thinned epoxy-impregnated sections which had been cut, ground and polished according to standard metallographic practices to a thickness of approximately 30 μm. A Gatan ion-miller was employed and the conditions used were 5 to 6 keV, 1 mA gun current, and 10 to 15° gun tilt using two guns. Specimen porosity and uneven specimen puncturing are the main problems encountered in ion-thinning, and only relatively small areas adjacent to milled holes could be viewed. TEM studies were undertaken using a Philips EM400 operated at 120 kV equipped with an EDS attachment, and an AEI EM-7 operated at 1 MeV.

3. Results and discussions

3.1. Differential thermal analysis (DTA)

The sensitivity of the instrument used in this study limited detection to the $\alpha'_H \rightleftharpoons \alpha$ transformation.

TABLE II Peak temperatures for the $\alpha'_H \rightleftharpoons \alpha$ transition on heating and cooling

Polymorph	Heating	Cooling
BaO β	1400° C	1376° C
BaO α'	1320° C	1304° C
B_2O_3 β	1396° C	1368° C
B_2O_3 α'	1310° C	1270° C
P_2O_5 β	1220, 1280° C	1186° C
P_2O_5 α'	1094° C	1080° C

The peak temperatures for this transformation for the different polymorphs are listed in Table II. The results indicate that the transformation temperature is reduced with increasing stabilizer content which has also been noted by Matković *et al.* [8]. This is indicative of the dopant entering the C_2S lattice in solid solution, which is in accord with known behaviour [1, 2]. The P_2O_5-doped β-C_2S showed a double peak on cooling (but not on heating) as has also been reported by Matković *et al.* [8]. The reason for this is not known.

3.2. Scanning electron microscopy (SEM)

All of the β-C_2S preparations contain grain boundary phases and reveal lamellae within the grains which correspond to the type II crystals in Insley's classification [15, 16]. Fig. 1 depicts a P_2O_5-doped β-C_2S sample lightly etched (5 sec) with 0.5% nital showing the characteristic lamellae. There is also an indication of a linear array of precipitates (marked with arrows). Grain boundaries (marked L) of varying widths and characteristics are also visible. Longer etching erodes the grains preferentially, leaving the boundary phase in high relief. Similar observations are also made for B_2O_3- and BaO-doped β-C_2S [14]. The P_2O_5- and B_2O_3-doped α'-C_2S samples show small grains with a few large ones which do not reveal much surface detail on etching. On the other hand, BaO-doped α'-C_2S show the cross-striations in the grains (type I according to Insley [15, 16]) observed previously by optical microscopy [9], and also a grain boundary phase, Fig. 2. As with the β-C_2S preparations, the grains are attacked preferentially during etching with nital.

3.3. Electron microprobe analysis (EMPA)

The starting compositions of the different preparations and the corresponding probe analyses are presented in Table I. Most often the grain boundary phases are of dimensions such that excitation of surrounding grains also takes place which make quantitative analysis very difficult. Qualitative estimates of elemental segregation between grains and

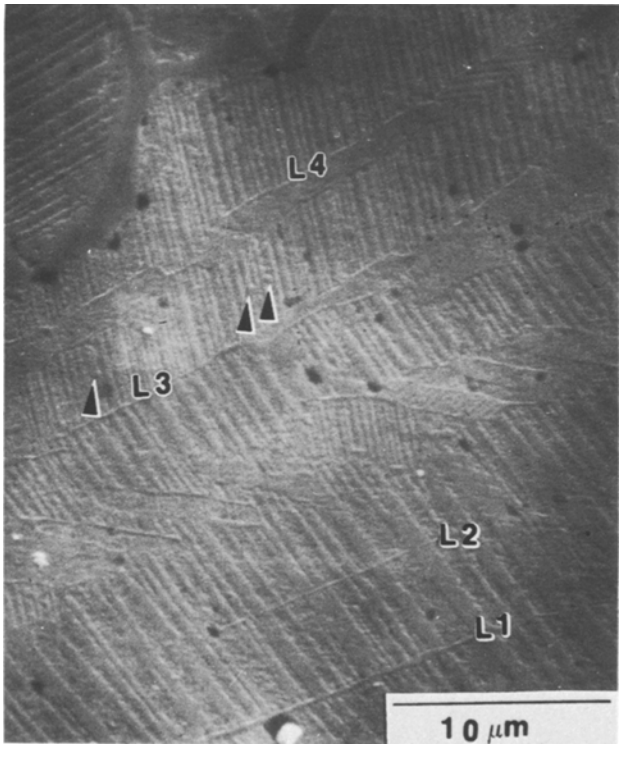

Figure 1 SEM micrograph of P_2O_5-doped β-C_2S etched for 5 sec with 0.5% nital. Arrows mark a linear array of precipitates. Grain boundaries marked with L.

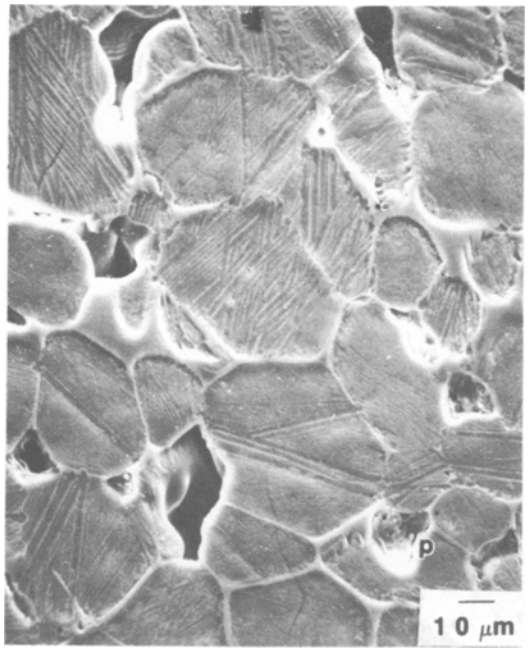

Figure 2 SEM micrograph of BaO-doped α'-C_2S etched for 15 sec with 0.5% nital. p denotes a pore.

grain boundaries were, however, made for BaO-doped α'- and β-C_2S: the grain boundaries were decidely richer in barium and had a lower Ca/Si count ratio than for the grains. For P_2O_5-doped β-C_2S, the grain boundaries had lower Ca/Si ratios than the grains, but segregation of phosphorus in the grain boundaries was not observed. Both grains and grain boundaries in B_2O_3-doped β-C_2S had similar Ca/Si ratios, but boron could not be detected by EDS. It has also been found that the grain boundaries frequently contain appreciable quantities of aluminium, which was presumably acquired during the specimen preparation stages, and apparently concentrates in the grain boundaries rather than the grains. For BaO- and P_2O_5-doped α'- and β-C_2S grains, the EMPA analyses indicate CaO/SiO_2 ratios fairly similar to the starting compositions after accounting for the major substitutions. Although for the individual components divergences from the starting compositions do occur, these differences are usually rather small. For P_2O_5 doping there is the additional chance of loss of some phosphorus during firing. Calculation of CaO/SiO_2 ratios for the B_2O_3-doped β- and α'-C_2S grains from EMPA results is more uncertain on account of the inability of detection of both boron and oxygen.

3.4. Transmission electron microscopy (TEM)

The TEM studies were undertaken to gain an insight into the composition and crystallinity of the grains, the grain boundary phases, any precipitates present within the grains and also generally to examine the microstructure at higher magnifications. The results are discussed separately under β-C_2S and α'-C_2S headings.

3.4.1. β-C_2S

Photomicrographs of P_2O_5-stabilized β-C_2S are illustrated in Figs. 3 to 5. Lamellae characteristic of β-C_2S are seen in Figs. 3 and 4. The arrows indicate some "split" lamellae which are joined some distance away, which might be construed to imply that either the larger lamellae splits into smaller ones or that smaller lamellae coalesce to form the larger lamella. Similar features have also been seen for β-C_2S doped with BaO or B_2O_3. The inset in Fig. 3 is the diffraction pattern from the area, which clearly displays (100) reflection twinning. Similar (100) twinning has also been seen in the other β preparations consistent with the structure of β-C_2S [17]. Although (001) twinning is also possible crystallographically, no instances of this were found, in agreement with Groves' [18] findings. Fig. 4 also depicts a boundary between adjacent grains, but does not display a distinct grain boundary phase, as seen in Fig. 5. Instead, dislocation tangles are evident at the boundary as well as inside the lamellae. The grain boundary phase (A) in Fig. 5 is amorphous, as deduced from its inability to diffract; this is also true for the other β-C_2S preparations. TEM-EDS analyses of these grains and grain boundaries are in close agreement with microprobe results (Section 3.3).

Fig. 6, from B_2O_3-doped β-C_2S, indicates a twin domain with the lamellae above and below the domain appearing to be parallel to each other. Dislocations and indication of a second phase at the domain boundaries can also be seen. A similar domain structure has been reported by Groves [18], who attributes its formation to a shear transformation as the specimen cools from the α to the β phase field. However, such domain structures have not been observed for the P_2O_5- or BaO-doped β-C_2S samples.

3.4.2. α'-C_2S

α'-C_2S doped with P_2O_5 does not display any distinguishing feature in the grains and no second

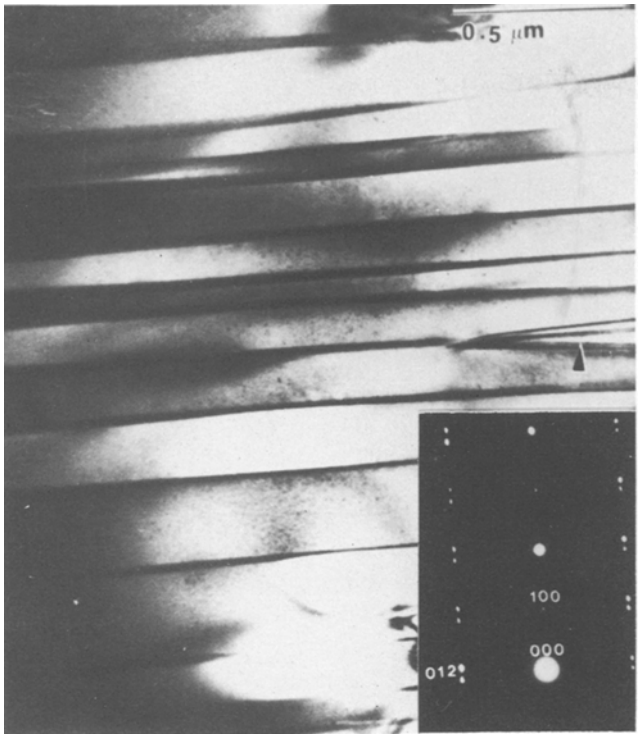

Figure 3 TEM micrograph of P_2O_5-doped β-C_2S. The arrow shows a split lamella. Inset is the diffraction pattern showing [100] twinning.

Figure 4 TEM micrograph of P_2O_5-doped β-C_2S. Dislocations (d) are visible at the grain boundary.

Figure 5 TEM micrograph of P_2O_5-doped β-C_2S showing grain boundary phase (A) and grain (B).

Figure 6 TEM micrograph of B_2O_3-doped β-C_2S showing a domain structure.

Figure 7 TEM micrograph of BaO-doped α'-C_2S showing grain boundary phase (A), grain (B) and precipitates (p).

phases have been observed. Typical results for BaO-doped α'-C_2S are shown in Figs. 7 to 10. Fig. 7 is a TEM micrograph, while Fig. 8 is an equivalent SEM micrograph, although not from the same area. Both display a grain boundary phase and presence of precipitates between the striae. The scale of magnification is, however, quite different, which would indicate the presence of similar microstructural features over a wide range of sizes. This has also been observed in the case of β-C_2S. Fig. 9 shows precipitates in the α'-C_2S grain. These are rich in barium, evidenced from TEM-EDS spectra, and appear to be exsolutions formed during quenching of the specimen. In most of the regions they are in linear arrays whereas in some they are random. Associated lobes of contrast can often be

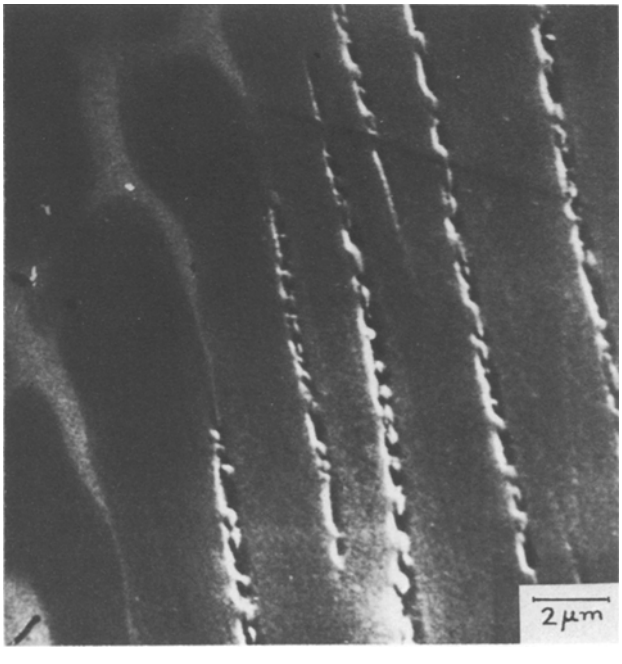

Figure 8 SEM micrograph of a similar area in BaO-doped α'-C_2S.

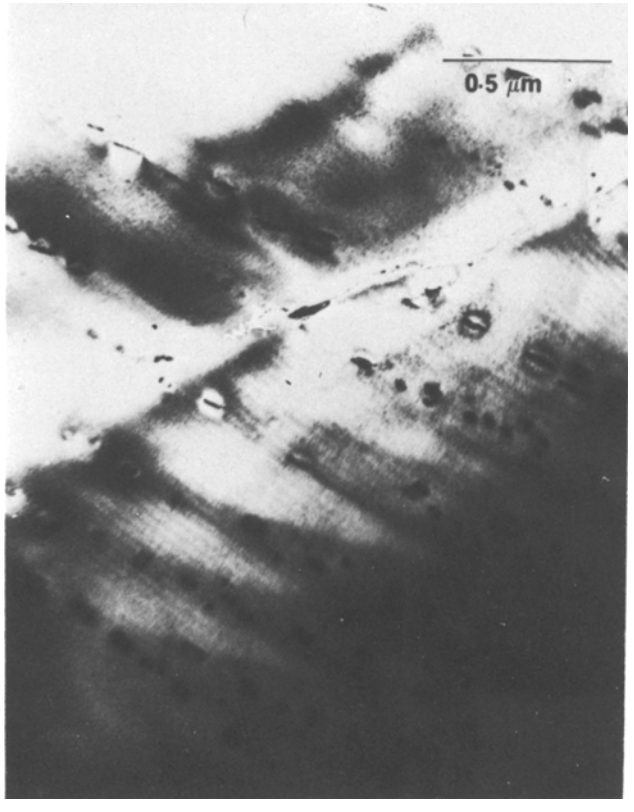

Figure 9 TEM micrograph of BaO-doped α'-C_2S showing precipitates with attendant lobes of contrast.

observed suggesting a lattice mismatch between the grain and the precipitates. Fig. 10 depicts a linear array of precipitates with associated dislocation tangles. Two sets of arrays meeting at an angle is suggestive of a grain boundary, although no distinct boundary is observed. The diffraction pattern from an area of this sample exhibited superstructure spots indicative of a tripling of the c-axis, commensurate with α'_L-phase [19], and also reported by Jelenić and Bezjak [20] for samples stabilized with sodium phosphate; apparently it is possible to have both α'_L and α'_H phases stabilized in a sample depending on the cooling history of various areas.

The microstructure of B_2O_3-doped α'-C_2S is very similar (Fig. 11) to the BaO-doped specimen. Linear arrays of precipitates are visible, their density being in general less than that for the BaO sample. A distinct contrast is exhibited between the precipitate rows and the matrix which might suggest there is a thickness variation between these areas. This variation could occur during the ion-milling process if the precipitates are harder than the matrix. The precipitates could not be analysed as to their chemical compositions. No distinct grain boundary phase was detected in this sample.

The TEM examination suggests that there is a higher precipitate density and attendent dislocations for the BaO-doped α'-C_2S, in the sample studied, whereas no precipitations were observed for P_2O_5-doping. Since lattice strains and dislocations contribute significantly towards reactivity, it might be conjectured that the reactivities would decrease in the order α'-C_2S(BaO) > α'-C_2S(B_2O_3) > α'-C_2S(P_2O_5). Matković [21] and Jelenić and Bezjak [22] have indeed observed that α'-C_2S(BaO) is more reactive than either of the other two, but a comparison of reactivities between B_2O_3-doped and P_2O_5-doped α'-C_2S has yet to be made.

4. Conclusions

The microstructure of the β-C_2S preparations were similar regardless of the dopant used. The lamellae are of different widths and exhibit splitting in some areas; they arise from twinning along the (100) plane. Domain structures were observed. Amorphous grain boundary phases were observed

Figure 10 HVTEM micrograph of BaO-doped α'-C_2S showing linear arrays of precipitates and dislocation tangles.

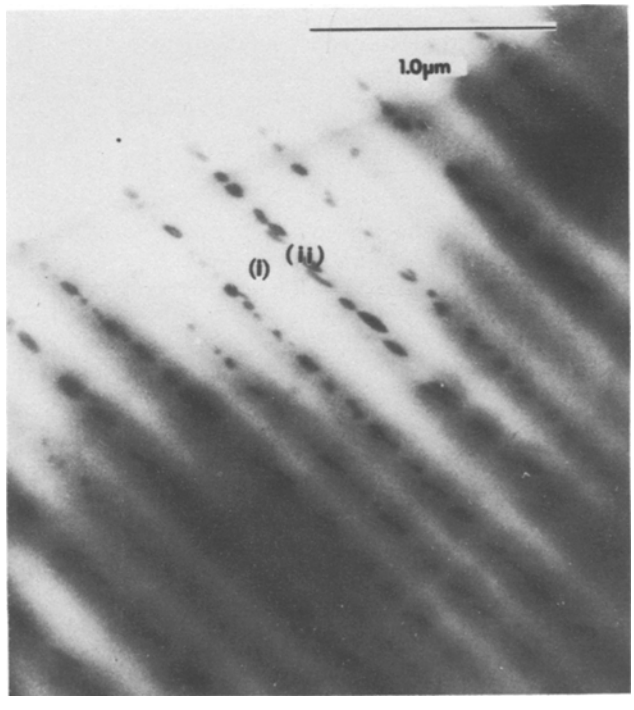

Figure 11 TEM micrograph of B_2O_3-doped α'-C_2S showing linear arrays of precipitates.

in every preparation, but the dopant does not necessarily concentrate in this phase. Barium enrichment was shown to occur by microprobe and EDS analyses whereas an absence of phosphorus was established in the same way. Alumina impurities also concentrated in the grain boundary phase. Not every grain boundary has a second phase present, in its absence dense dislocation tangles are observed.

Only BaO-doped α'-C_2S showed a distinct grain boundary phase, also rich in barium. This preparation had extensive arrays of precipitates within the grain which are manifested as boundaries between the cross-striations observable by SEM and optical microscopy. These precipitates have been shown to be rich in barium which are thought to be exsolutions. Their associated dislocation tangles and strain fields probably account for the greater reactivity of BaO-doped α'-C_2S. Similar arrays of precipitates are observed in B_2O_3-doped α'-C_2S, but their density is less and fewer dislocations were observed. Such features are entirely absent in P_2O_5-doped α'-C_2S preparations.

Acknowledgements

This work was supported by the National Science Foundation, Grant No. CEE-22068. The use of the facilities of the Center for Microanalysis, Materials Research Laboratory, and of the Center for Electron Microscopy at the University of Illinois is gratefully acknowledged. The use of HVEM facilities at Argonne National Laboratory is also acknowledged with thanks. The work performed by S.C. was in partial fulfillment of the MS degree in Ceramics at the University of Illinois.

References

1. S. N. GHOSH, P. B. RAO, A. K. PAUL and K. RAINA, *J. Mater. Sci.* **14** (1979) 1554.
2. M. REGOURD and A. GUINIER, Proceedings of the 6th International Congress on the Chemistry Cements, Moscow, 1974, Principal Paper (English Preprint). Russian Edition Stroizdat, 1975.
3. P. BARNES, C. H. FENTIMAN and J. W. JEFFEREY, *Acta Crystallogr.* **A36** (1980) 353.
4. V. I. KORNEEV and E. B. BYGALINA, Proceedings of the 5th International Symposium on the Chemistry of Cements, Tokyo, 1968 (Cement Assocation Japan, Tokyo, 1969) **I**, 285.
5. J. STARK, A. MÜLLER, R. SCHRADER, K. RÜMPLER and B. DAHM, *Silikattechnik* **30** (1979) 357.
6. *Idem, ibid.* **31** (1980) 50, 168.
7. K. SUZUKI, S. ITO, S. SHIBATA and N. FUJII, Proceedings of the 7th International Congress on the Chemistry of Cement, Paris, June 1980, Vol. 2 (Editions Septima, Paris, 1980) II-47.
8. B. MATKOVIĆ, V. CARIN, T. GAČEŠA and R. HALLE, Proceedings of the 7th International Congress on the Chemistry of Cements, Paris, June 1980, Vol. 2 (Editions Septima, Paris, 1980) I-189.
9. B. MATKOVIĆ, V. CARIN, T. GAČEŠA, R. HALLE, I. JELENIĆ and J. F. YOUNG, *Amer. Ceram. Soc. Bull.* **60** (1981) 825.
10. B. BOBESIĆ, R. HALLE, M. MIKOĆ, B. MATKOVIĆ and J. F. YOUNG, *ibid.* **60** (1981) 1164.
11. S. CHOPRA, MS thesis, University of Illinois, Urbana, USA (1982).
12. K. SUZUKI and G. YAMAGUCHI, Proceedings of the 5th International Symposium on the Chemistry of Cement, Tokyo, 1968 (Cement Association Japan, Tokyo, 1969) **I** 67.
13. I. JELENIĆ, A. BEZJAK and M. BUJAN, *Cem. Concr. Res.* 8 (1978) 173.
14. S. CHOPRA, A. GHOSE and J. F. YOUNG, Proceedings of the 5th International Conference in Cement Microscopy, Nashville, TN, March 1983, in press.
15. H. INSLEY, *J. Res. Nat. Bur. Stand.* **17** (1936) 353.
16. *Idem, ibid.* 25 (1940) 295.
17. C. M. MIDGLEY, *Acta Crystallogr.* **5** (1952) 307.
18. G. W. GROVES, *Cem. Concr. Res.* **12** (1982) 619.
19. H. SAALFELD, *Amer. Mineral.* **60** (1975) 824.
20. I. JELENIĆ and A. BEZJAK, *Cem. Concr. Res.* **12** (1982) 785.
21. B. MATKOVIĆ, "Development of Strength in Cement," FHWA Report RD-80/180, 132p, Fed. Highway Admin., Washington, DC, April, 1981.
22. I. JELENIĆ and A. BEZJAK, *Cem. Concr. Res.* **11** (1981) 467.

Received 13 January
and accepted 10 February 1983